

Article

Cable Connection Optimization for Heterogeneous Offshore Wind Farms via a Voronoi Diagram Based Adaptive Particle Swarm Optimization with Local Search

Yuanhang Qi ^{1,2}, Peng Hou ^{3,*}, Guisong Liu ^{1,2}, Rongsen Jin ⁴, Zhile Yang ⁵, Guangya Yang ⁶ and Zhaoyang Dong ⁷

- ¹ School of Computer Science, University of Electronic Science and Technology of China, Zhongshan Institute, Zhongshan 528402, China; qiyuanhang@zsc.edu.cn (Y.Q.); lgs@uestc.edu.cn (G.L.)
² School of Computer Science and Engineering, University of Electronic Science and Technology of China, Chengdu 611731, China
³ SEWPG European Innovation Center, 8000 Aarhus, Denmark
⁴ Department of Operation, University of Groningen, 9747 Groningen, The Netherlands; jinrongsen@outlook.com
⁵ Shenzhen Institute of Advanced Technology, Chinese Academy of Sciences, Shenzhen 518055, China; zl.yang@siat.ac.cn
⁶ Center of Electric Power and Energy, Department of Electrical Engineering, Technical University of Denmark, 2800 Lyngby, Denmark; gyy@elektro.dtu.dk
⁷ School of Electrical Engineering and Telecommunications, University of New South Wales, Sydney, NSW 2052, Australia; joe.dong@unsw.edu.au
* Correspondence: houpeng@shanghai-electric.com



Citation: Qi, Y.; Hou, P.; Liu, G.; Jin, R.; Yang, Z.; Yang, G.; Dong, Z. Cable Connection Optimization for Heterogeneous Offshore Wind Farms via a Voronoi Diagram Based Adaptive Particle Swarm Optimization with Local Search. *Energies* **2021**, *14*, 644. <https://doi.org/10.3390/en14030644>

Academic Editor: Jose Palma

Received: 16 December 2020

Accepted: 22 January 2021

Published: 27 January 2021

Publisher's Note: MDPI stays neutral with regard to jurisdictional claims in published maps and institutional affiliations.



Copyright: © 2021 by the authors. Licensee MDPI, Basel, Switzerland. This article is an open access article distributed under the terms and conditions of the Creative Commons Attribution (CC BY) license (<https://creativecommons.org/licenses/by/4.0/>).

Abstract: Offshore wind energy, as one of the featured rich renewable energy sources, is getting more and more attention. The cable connection layout has a significant impact on the economic performance of offshore wind farms. To make better use of the wind resources of a given sea area, a new method for optimal construction of offshore wind farms with different types of wind turbines has emerged in recent years. In such a wind farm, the capacities of wind turbines are not identical which brings new challenges for the cable connection layout optimization. In this work, an optimization model named CCLOP is proposed for such wind farms. The model incorporates both the cable capital cost and the cost of power losses associated with the cables in its objective function. To get an optimized result, a Voronoi diagram based adaptive particle swarm optimization with local search is proposed and applied. The simulation results show that the proposed method can help find a solution that is 12.74% outperformed than a benchmark.

Keywords: offshore wind farm; multiple wind turbine types; cable connection layout; power losses; Voronoi diagram; adaptive particle swarm optimization; local search

1. Introduction

With the increasing demand for green energy, the use of rich renewable energy sources such as wind energy has drawn a wide attention [1]. Compared with onshore wind farms, offshore wind farms (OWFs) possess superiorities involving higher wind speed, rich wind energy resources, less turbulence intensity, good visualization, noise-free to residents, etc. [2]. However, the immense investment, including capital expenditure (CAPEX) and the operational cost of OWFs, is much higher than that of onshore wind farms, which seriously hinders their commission and development [3]. Therefore, in order to obtain an OWF with high investment benefits, researchers are devoted to studying the cable connection layout optimization problem (CCLOP) of OWFs [4]. Based on the concept of the minimum spanning tree (MST) in graph theory, the greedy algorithm has been used to solve the CCLOP [5]. In [5], the whole wind farm was divided into several regions using the fuzzy c-means algorithm, then the Prim algorithm is used to solve the CCLOP for each area. Due

to the complexity of the CCLOP, metaheuristic algorithms were also adopted to solve the CCLOP [6,7]. In [6], the optimization model of the CCLOP is established considering the voltage level, quantity, and location of the offshore substation (OS), then the model was solved by the genetic algorithm. In [7], a new model based on the concept of MST was proposed and solved by the adaptive particle swarm optimization (APSO) algorithm. The simulation result showed that the APSO outperformed the result obtained by the prime algorithm and the proposed dynamic MST algorithm. However, the influence of the cable energy losses cost (CELC) [8] on the cable connection layout is not considered in the above work.

With the increasing capacity and distance to shore of offshore wind farm, the CELC becomes increasingly significant for CCLOP [8]. To consider this factor, some studies have been conducted. In [9], a hybrid immune genetic algorithm was proposed to solve the CCLOP. The cost of more components such as transformers and substations was considered simultaneously with the cables' costs and solved by an improved genetic algorithm in [10]. In addition to using heuristic and metaheuristic algorithms, mathematical programming was also applied in solving CCLOP considering CELC's impact [11,12]. In [11], the ordinal optimization and mixed-integer programming method were combined to solve the CCLOP and the results demonstrated that combined method obtains a better solution than mixed-integer programming. The CCLOP was formulated as mixed-integer linear programming problem in [12]. It was designed to ensure an uncrossed cable connection layout so as to eliminate the extra cots on installation as well as operations and maintenance.

On the other hand, existing OWFs are always composed of the same type of wind turbine (WT) whereas several recent studies have shown the benefits of constructing an OWF with diverse types of WTs [13,14]. Therefore, with the willingness of maximizing the use of the resources of the sea area, reducing the leveled cost of energy of the OWF, a new type of OWF, namely, an offshore wind farm with different wind turbine types (OWFD) came into being and attracted the worldwide attention. Reference [15] is one of the earliest studies on solving the wind farm layout optimization problem for an OWFD where the WTs positions and the type on each position were optimized simultaneously to maximize the total power generation. Similarly, the WTs' positions and the type based on the Jensen wake model to minimize the leveled cost of energy considering the cost of the foundation system, offshore electrical system, offshore transportation and installation in [16]. A 3D wake model for complex terrain was established in [17] while the WT micro-siting problem was solved by the greedy algorithm considering installing WTs with different hub heights.

However, the above literature only concerns the micro-siting optimization of the OWFD. To our knowledge, our work is the first to put forward a method for solving the CCLOP of the OWFD. The CCLOP of OWFD aims to optimize the cable connection while meets all the technical and engineering constraints, which is an intractable combinatorial optimization problem. The exact algorithms face the challenges of ensuring a feasible solution to such a problem [18]. In comparison, meta-heuristic algorithms find suboptimal solutions in an acceptable time, and have been adopted in many works [19,20]. Ref. [19] proposed a technique of coding the topology to a binary string and apply genetic algorithm to solve the CCLOP considering both middle and high-voltage alternating-current grids. Considering the wake effect and accurate power losses calculation method, ref. [20] proposed solved by an APSO to solve the CCLOP.

According to our previous work, the proximity relationship between WTs is important in obtaining an optimal cable connection layout. To give gain a better judgement of the the proximity relationship between the vertices (i.e., OS or WTs) and thus find a better solution, the Voronoi distance [21,22] is introduced to define the proximity relationship between vertices, and the two adjacent vertices are connected preferentially to improve the searching efficiency of the algorithm in this paper. Voronoi distance has achieved good results in vehicle routing problem optimization [23], and our work is the first to incorporate the Voronoi distance into the CCLOP model.

The main contribution of this work is summarized in the following:

- (1) Considering the influence of CELC on the economic performance, a CCLOP model of OWFD is established. To the best of our knowledge, this is the first work that proposes an optimization model for solving the CCLOP of OWFD.
- (2) To resolve the CCLOP, a novel V-APSO-LS algorithm is proposed, which adopts a K-ring shaped Voronoi neighbor (KSVN) and a local search strategy (LSS) to enhance the optimization ability of APSO.
- (3) The proposed algorithms are well verified via two case studies.

The remaining of this paper is organized as follows: Section 2 describes the CCLOP of OWFD. Section 3 provides a V-APSO-LS algorithm to solve the model. A wind farm with 72 WTs is chosen as the study case to demonstrate the proposed method and its strategies in Section 4. Some conclusions and future work on OWFD are given in Section 5.

2. Mathematical Models

In this section, the assumptions associated with the model are introduced at first. A new CCLOP model is specified which is established according to the characteristics of OWFD.

2.1. Assumptions

To make the paper more readable, some corrections have been made for the assumption section in the following.

- The type of WT in each position within the wind farm is given which is also the truth that the CCLOP was solved after the micro-siting of wind turbines were decided.
- To simply the cable length calculation, the distance between the OS and the WTs is a two-dimensional Euclidean distance. In reality, this length is always modified by a redundancy factor.
- All WTs are assumed to be operated at 1 p. u. voltage and the power factor is assumed to be 0.95.

Based on the above assumptions, this article will establish an optimization model of CCLOP based on OWFD.

2.2. Optimization Model

2.2.1. Objective Function

In graph theory, a spanning tree is a subgraph of an undirected graph G [7]. The subgraph contains all vertices and some branches in G . All vertices have paths to communicate with each other, but there are no loops. The spanning tree of a weighted G can be expressed as:

$$G_T = (V, B_T, W_T), G_T \in G, B_T \in B, W_T \in W \quad (1)$$

where V represents the set of all vertices, B is the set of all branches connecting the vertices in V . W is the set of weights corresponding to all branches in B . G_T is a subgraph of G , representing a spanning tree of G . Similarly, B_T is the set of the branches in B while W_T is the weight corresponding to all branches in B_T .

According to the definition of the spanning tree shown above, we know that if the OS (represented by V_{OS}) and WTs (represented by V_{WT}) are regarded as the vertices of G , the cost of the cable connecting the two vertices (between OS and WT or WT and WT) is the weight of the branch. Then the CCLOP problem can be transformed into a mathematical problem of finding a G_T with minimum total weight in a weighted G . The objective function of the CCLOP problem includes two parts: CAPEX of cables and CELC, of which the detailed mathematical expressions are discussed in the following sections.

The cost of CAPEX of branch m with cable type p is calculated as:

$$Z_{CAPEX,G_T,m,p} = C_p L_{G_T,m} \varphi_{G_T,m,p} \quad (2)$$

Then, the total cost of CAPEX of all cables can be formulated as:

$$Z_{CAPEX,G_T} = \sum_{m=1}^M \sum_{p=1}^P Z_{CAPEX,G_T,m,p} \quad (3)$$

In addition, the power losses along the cables reduce the profits of the wind farm owner and appear all over the lifetime of the offshore wind farm. In order to account for it, the net present value of the CELC during the wind farm's lifetime is incorporated into the objective function as follows:

$$Z_{CELC,G_T,m,p} = (I_{G_T,m,p})^2 R_p L_{G_T,m} \varphi_{G_T,m,p} \quad (4)$$

where $I_{G_T,m,p}$ is the sum of currents flowing through the branch m . In a homogeneous wind farm, the power through the cable is usually calculated according to the total number of WTs that the cable undertaken which has been adopted in [7,12,20,24]. In an OWFD, the rated powers of WTs are not identical. In order to calculate the power flow in each cable when all the WTs are in full load condition, the WTs' types associated with the cable should be identified. A simple example is shown to explain how the $I_{G_T,m,p}$ is calculated in such a case.

Supposing that there are two offshore wind farms with the same layout (one OS and four WTs are with the same coordinates). One is the homogeneous wind farm which composed of the same type of WTs while the other one is the OWFD. All the WTs in each wind farm are operated in full load condition. The rated power for type one and two WT is 2 MW and 3 MW, respectively. Neglecting the power losses, the actual power along each branch are compared in Figure 1.

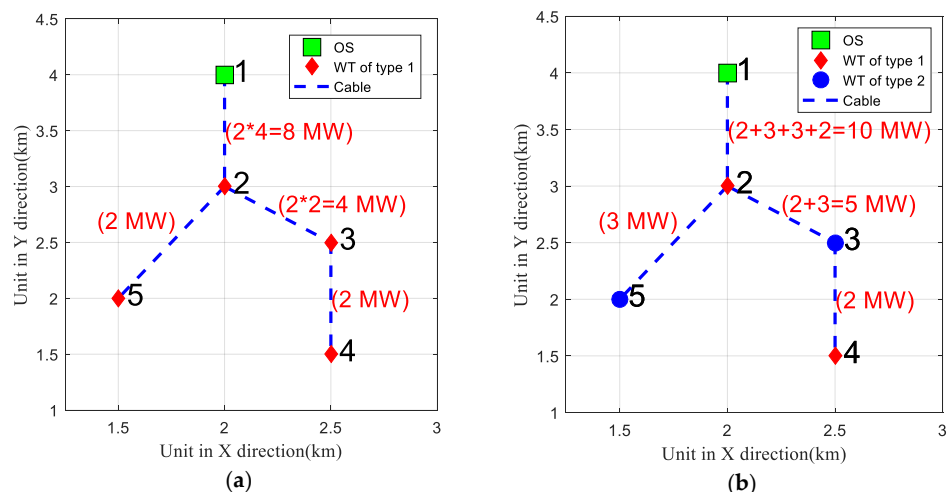


Figure 1. A simple example of Energy calculation when all WTs are operated in full load condition. (a) Energy distribution for the homogeneous wind farm; (b) Energy distribution for the OWFD.

In Figure 1a, there are four WTs transmitting their energies to cable (1,2), which has the same type. Therefore, the actual carrying capacity of cable (1,2) in Figure 1a is $4 \times 2 = 8$ MW. In Figure 1b, the WTs transmitting energies to cables (1,2) include two type 1 WTs and two type 2 WTs. Therefore, the actual power reached at the cable (1,2) in Figure 1b is $2 + 3 + 3 + 2 = 10$ MW. It can be seen that when there is only one type of WTs in the wind farm, it can be obtained by the product of the number of WTs transmitting energies to the cable and the rated WT's power. However, if the WTs in the wind farm are not identical, the corresponding WT types and number of each type of WTs related to the cable should

be identified so that the actual power of each cable can be calculated. As a result, Equation (5) is modified to resolve the above issue:

$$I_{G_T,m,p} = \sum_{h=1}^{H_{G_T,m}} I_{rate,q} \delta_{G_T,q,h} \quad (5)$$

where $H_{G_T,m}$ is the number of the WTs that transmit their power through the branch m of G_T while $I_{rate,q}$ is decided by the WT type q , the mathematical expression is written as:

$$I_{rate,q} = \frac{P_{rate,q}}{\sqrt{3} \cos \psi U_{rate,q}} \quad (6)$$

Then the CELC of all cables can be written as:

$$Z_{CELC,G_T} = 3 \times \sum_{\xi=1}^T (1 + \eta)^{\xi} \psi_{\Delta} C_{loss} \left(\sum_{m=1}^M \sum_{p=1}^P Z_{CELC,G_T,m,p} \right) \quad (7)$$

Finally, the overall objective function is defined as:

$$Z_{min,total} = \min(Z_{CAPEX,G_T} + Z_{CELC,G_T}) \quad (8)$$

2.2.2. Constraints

The main constraints involve in this work are summarized in the following:

$$G_T \in G \quad (9)$$

$$I_{G_T,m,p} \leq I_{max,p}, \forall m = 1, 2, \dots, M, \forall p = 1, 2, \dots, P \quad (10)$$

$$1 \leq F_{G_T,V_{OS,in}} \leq 10, V_{OS} \in V \quad (11)$$

$$1 \leq F_{G_T,V_{WT,m,in}} \leq 2, \forall V_{WT}, m \in V_{WT}, \forall m = 1, 2, \dots, M \quad (12)$$

$$F_{G_T,V_{WT,m,out}} = 1, \forall V_{WT}, m \in V_{WT}, \forall m = 1, 2, \dots, M \quad (13)$$

$$\forall B_{m1} \cap B_{m2} = \emptyset, B_{m1} \in B_T, B_{m2} \in B_T, m1 \neq m2 \in [1, M] \quad (14)$$

Equation (9) is to ensure that G_T is a spanning tree of G . Based on the principle of equipment protection, the actual current flowing through each cable cannot exceed its maximum current carrying capacity which is constrained in Equation (10). From the engineering point of view, some constraints are made from Equations (11)–(13) which represents the maximum number of cables that an offshore substation can hold, the number of incoming cables for each WT, and the number of outgoing cables for one WT respectively. The crossed cables would not only endanger the operation of OWF but also increase the installation cost. To ensure an uncrossed cable connection layout, Equation (14) is added to this work.

3. Proposed Optimization Method

In this section, a novel V-APSO-LS algorithm is proposed for solving the above intractable problem. The canonical APSO algorithm structure is specified at first. Secondly, a simple example is elaborated to show how the k-ring shaped Voronoi neighbor-based model is created. Then, the local search enhanced APSO is shown. The overall framework of the V-APSO-LS is specified in the end.

3.1. APSO Algorithm

As one of the population-based methods, particle swarm optimization was firstly proposed by Kennedy and Eberhart for solving a continuous nonlinear problem [25,26]. It is a random search algorithm based on group cooperation, which is developed by simulating

the foraging behavior of birds. In this algorithm, particles have two properties: speed and position. The speed of the particles represents the speed of movement, and the position of the particles represents the current solution. The algorithm finds the optimal solution by updating the speed and position of the particles, which can be expressed as:

$$v_{i,t+1} = \omega \cdot v_{i,t} + r_1 \cdot \text{rand}() \cdot (LB_{i,t} - x_{i,t}) + r_2 \cdot \text{rand}() \cdot (GB_{i,t} - x_{i,t}) \quad (15)$$

$$x_{i,t+1} = x_{i,t} + v_{i,t+1} \quad (16)$$

where the first term in Equation (15) is a weighting factor, the second term is a cognitive learning part, and the third term is a social learning part. The later research [27] found that the larger the w is, the stronger the global optimization searching ability that the algorithm has, and thus shows a weaker the local optimization searching ability; if it gets smaller, the algorithm's local optimization ability is stronger, and the global optimization ability is weaker. It can be seen that the global and local optimization searching performance of the algorithm can be adjusted by tuning the parameters. In the light of this, an APSO with a non-linear reduction of inertia weight was proposed in [27]. The weight was changed according to the following rule:

$$\omega = \frac{1}{1 + 1.5e^{-2.6\mu}} \in [0.4, 0.9], \forall \mu \in [0, 1] \quad (17)$$

$$\mu = \frac{d_{avg} - d_{min}}{d_{max} - d_{min}} \quad (18)$$

According to our previous work [7,20,28], APSO with initial values of $r_1 = 2$, $r_2 = 2$ and $\omega = 0.9$ has shown good performance in solving CCLOP compare with MST. Furthermore, as indicated in [29], particle swarm optimization has higher computation efficiency in solving non-linear problem compared with other meta-heuristic algorithms. Therefore, the APSO is selected as the core algorithm to optimize CCLOP in this work.

3.2. V-APSO-LS Algorithm

In this section, a new coding and decoding strategy based on k-ring shaped Voronoi neighbor and APSO, named V-APSO-LS, is proposed. In order to further enhance the local search ability of the algorithm, a random local search strategy is incorporated and specified at last.

3.2.1. K-Ring Shaped Voronoi Neighbor

A Voronoi diagram is a typical metric space decomposition method [22,30–32]. According to a nearest-neighbor rule, each discrete point in the Voronoi diagram is associated with the region of the plane close to it. Each discrete point corresponds to only one region. Due to the bisected features of the Voronoi diagram in spatial decomposition, it is often applied to solve the problems such as nearest points, adjacencies, and proximity. In 1991 Aurenhammer et al. proposed the definitions of the Voronoi diagram, Voronoi region, and Voronoi branches [30–32]. In 2017, Fang proposed the definition of k-ring shaped Voronoi neighbor [22]. In the following, the detailed definitions related to the Voronoi diagram are specified.

Definition 1. The discrete points distributed on the Voronoi diagram are defined as the Voronoi site. Hence, the WTs and OS are Voronoi sites in this work.

Definition 2. The corresponding Voronoi regions of the site E_1 and E_2 are $VR(E_1)$ and $VR(E_2)$ respectively. If there is a Voronoi edge between $VR(E_1)$ and $VR(E_2)$, then E_1 and E_2 are Voronoi neighbors. For instance, there are totally 29 Voronoi sites in Figure 2 while E_1 and E_2 are one pair of the Voronoi neighbors.

Definition 3. The Voronoi distance between E_1 and E_2 is defined as the number of Voronoi branch intersected by the line connecting E_1 and E_2 . For example, the Voronoi distance between E_1 and E_2 in Figure 2 is one.

Definition 4. The k -ring shaped Voronoi neighbors set of E_1 is referring to the set of k points with Voronoi distance from E_1 , denoted as $KN(E_1, k)$. For example, $KN(E_1, 1)$, $KSVN(E_1, 2)$ and $KN(E_1, 3)$ is the 1-ring, 2-ring, 3-ring Voronoi neighbors sets of E_1 which are shown in Figure 2, respectively.

As can be seen from Figure 2, the metric space is divided by the Voronoi diagram. Instead of judging two points' proximity relationship by the Euclidean distance, the Voronoi distance is obtained based on redefining the proximity relationship between the sites, which is a more scientific method of judging the proximity relationship [23]. The reason is that a shorter Euclidean distance two sites does not also mean that their proximity relationship is closer. A simple example is given in this work to illustrate the abovementioned situation, as shown in Figure 3.

In Figure 3, there is a wind farm with 1 OS and 5 WTs (totally 2 types of WTs). It can be seen that the Euclidean distance between the 6th node to the OS is closer than the distance between the 3rd node to the OS. However, the 3rd node is the 1st order neighbor of OS while the 6th node is the 2nd order neighbor of the 1st node. Hence, the 3rd node is a closer neighbor of OS compared with the 6th node. Similarly, the 4th node and 5th node are also the closer neighbors of OS compared with the 6th node. It can be seen that in generating the cable connection layout, when the WT connected to the OS needs to be selected, the priority of the 3rd node should be higher than the 6th node, and the 6th node should be connected to the 4th site or 5th node.

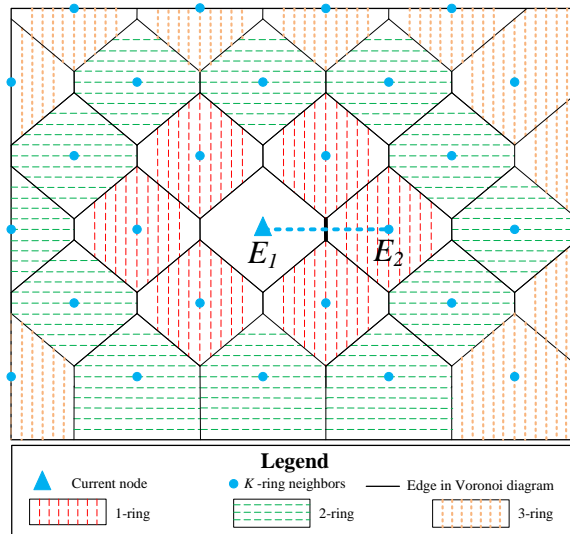


Figure 2. Voronoi diagram.

It can be seen that the Voronoi diagram judge the adjacent relationship between OS and WT, and between WT and WT in a wind farm more scientifically, which is conducive to selecting a better branch for cable connection in the layout process. The next section will introduce the KSVN based codec scheme, and elaborate on how to apply KSVN to cable connection layout optimization in this article.

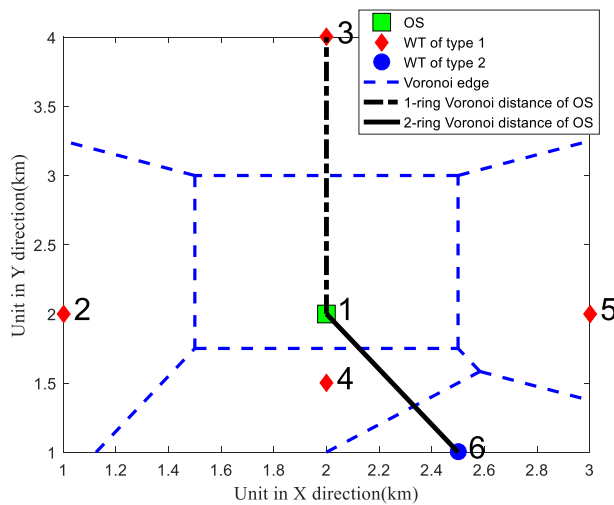


Figure 3. Voronoi diagram of a multiple wind turbine types offshore wind farms.

3.2.2. Encoding and Decoding of Particle

① Encoding of Particle

According to the model shown in Section 2, the algorithm in this paper does not only need to get the basic cable connection information, but also needs to consider the further influence of energy loss on the selection of cable type on the layout. Therefore, the particle code must contain two parts of information, one is the cable connection layout information, the other is the information of each cable type. Based on the above reasons, assuming the number of WTs is m , the particle i coding in this paper is shown in Figure 4.

Particle i position:									
Connection Index						CTIN Index			
S_1	S_2	\dots	S_m	\dots	S_M	S_{M+1}	S_{M+2}	\dots	S_{2M}

Figure 4. Encoding of particle i .

In Figure 4, $S_1 \dots S_M$ represent the connection index which belongs to $[1, m \times (M - m + 1)]$ and $m = 1, 2, \dots, M$ while $S_{M+1} \dots S_{2M}$ are the Cable Type Incremental Number (CTIN) index which are in the range of $[1, P]$.

② Decoding of Particle

Particle decoding includes two stages, the first stage is to get the cable connection information, and the second stage is to select the cable model according to the current cable connection information. In the whole decoding process, V-APSO-LS needs to use 6 basic sets and 3 matrices as follows:

- Set A: Including the vertices which have already been connected in MST.
- Set B: Including the vertices which have not yet been connected in MST.
- Set C: Including the length of each branch connecting vertices in set A.
- Set D: Including actual current of each branch in MST.
- Set E: Including the minimal cable type of each branch in MST.
- Set F: Including the final cable type of each branch in MST.

Adjacency matrix AM : Including all the Voronoi distance and the geometrical distance between each pair of adjacent stochastic vertices which are from set A and set B. Where set A is the index of the column and set B is the index of the row.

Sorted-adjacency matrix SAM : All the branches in the adjacency matrix AM are sorted from small to large according to the Voronoi distance. If the distance of two sides is equal,

the branches are sorted from small to large according to the length of the branch. Finally, the sorted-adjacency matrix SAM is obtained.

Cable matrix: Including the current carrying capacity, resistance and price per unit length for each type of cable, the cable data is arranged according to the ampacity of the cable from small to large.

In the first stage, set A only contains OS, set B contains all WTs, while set C, D, E and F are empty. First of all, according to the vertices of set A and B, the adjacency matrix is generated, and the branches in the adjacency matrix are sorted to get the sorted adjacency matrix. Then, V-APSO-LS selects a new branch according to the connection index of particle i and sorted adjacency matrix, and puts the branch related information into set C. At the same time, the vertices corresponding to the branch are deleted from set B and then put into set A. This phase will not end until set B is empty. It is worth noting that in the selection process of vertex and its corresponding branch, if the cable connection layout after the access of the branch does not meet the constraint from Equation (10) to Equation (14), the next branch in the sorted adjacency matrix is selected in order until the constraint is met. It should be noted that the new branch cannot cross the other branches in the spanning tree in each step which is just by the method specified in [2].

In the second stage, the actual power through each branch (i.e., cable) can be obtained according to the information in set C. The current passing through each branch (i.e., cable) will be calculated by Equations (5) and (6), and the current value is put into set D accordingly. Further, according to the current value in set D, the cable with the minimum current carrying capacity while meeting the constraint of Equation (10) will be selected [7], and put into set E. Finally, the selected cable type of each branch is decided according to the sum of the corresponding index in set E and the CTIN index of particle i which is the information that put into the set F. It is worth noting that if the added value exceeds the maximum index of the optional cable type, then the cable type will be set to the maximum cable type index.

To sum up, after two stages of decoding, the obtained information in set C and F can constitute a cable connection layout. Combined with set D, the corresponding cost of the cable connection layout can be calculated. In order to better explain the two stages of particle coding, an example is given in the following. It is assumed that there are totally six WTs with two types in the reference wind farm, the position of particle i is assumed to be [2,4,1,1,2,0,1,2,1,0]. There are three types of optional cable models (the larger the cable index, the greater the carrying capacity of the cable). Among them, the first five positions of the particle represent the connection index, and the last five positions represent the CTIN index. The detailed decoding process of particle i is shown in Figures 5 and 6 which represent the first and the second stages, respectively.

Assuming the position of particle i has been decoded the 1st dimension, and the current set A is [1,2], set B is [3,4,5,6], and set C is {{(1, 2), 1.00}}. Then, decoding the 2nd dimension of the particle i is shown in Figure 5. First, according to set A and set B, we get the adjacency matrix AM . Second, sorting all the branches in the AM from small to large according to the Voronoi distance, and then we get the sorted-adjacency matrix SAM . Third, because the value of the second dimension of particle i is four, the 4th branch (1,3) of the SAM is pointed. Lastly, assuming that the branch (1,3) satisfies the constraints from Equation (10) to Equation (14), then the relevant information of this branch will be put into set C. So the information in set C will be updated to {{(1,2),1.00}, {(1,3),2.00}}. Meanwhile, set A and set B are updated to [1,2,3] and [4,5,6] respectively. Similarly, the 3rd to 5th dimensions of the particle i can also be decoded according to the above steps and then set A will be created as [1,2,3,4,6,5] and set C as {{(1,2),1.00}, {(1,3),2.00}, {(1,4),0.50}, {(4,6),0.71}, {(4,5),1.12}}.

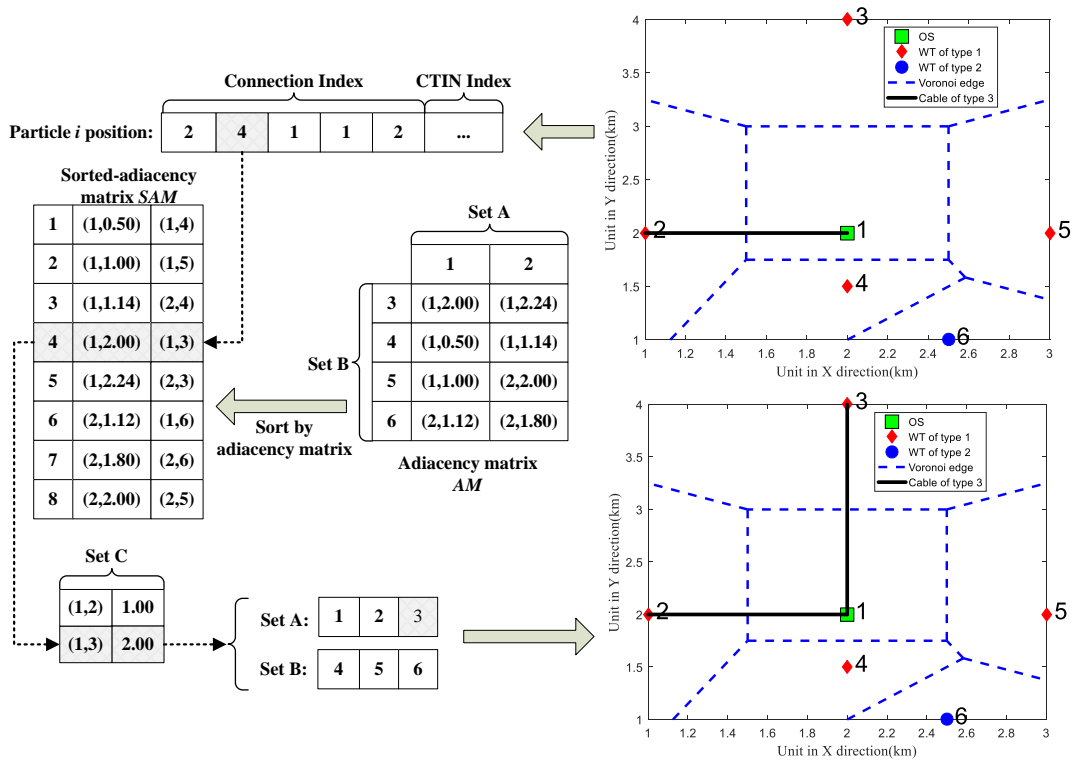


Figure 5. Decoding of particle (stage 1).

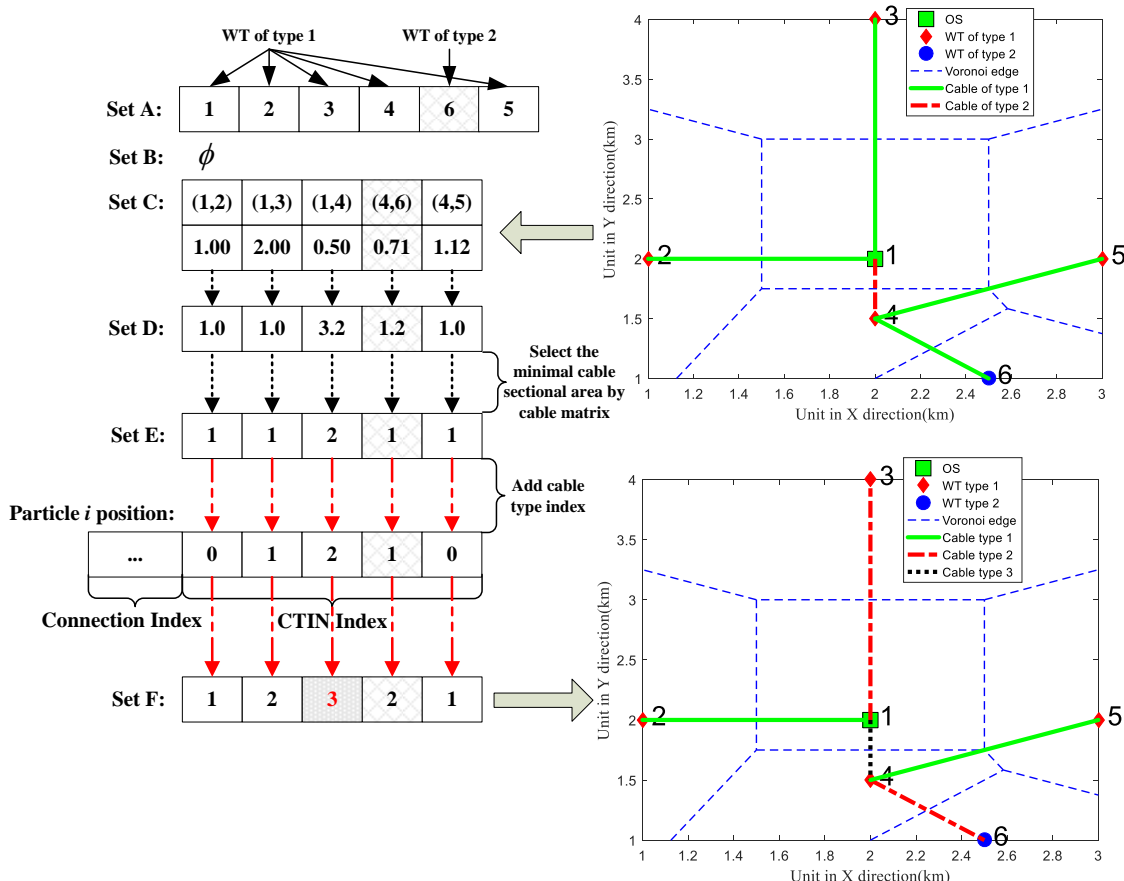


Figure 6. Decoding of particle (stage 2).

Next, the second stage of decoding is executed, as shown in Figure 6. First, according to the cable connection information of set C, set D that includes the current passing through each branch is calculated by Equations (5) and (6). Second, assuming set D is obtained as [1.0,1.0,3.2,1.2,1.0], under the rule of selecting the minimum current-carrying cable type, set E [1,1,2,1,1] is calculated. Third, the last five dimensions of the position of particle i are [0,1,2,1,0], as introduced above it should be added with the information in set E, so that the set F is initialized as [1,2,4,2,1]. However, since there is no cable with cable type 4, cable type 3 will be picked up and then set F becomes [1,2,3,2,1]. Finally, set C, set F and set D can get the cable connection layout corresponding to the particle i 's position and its related information.

3.2.3. Local Search Strategy

LSS is often used to improve the local optimization ability of the intelligent algorithm [33,34]. LSS directly optimizes the global optimal particles, and the updated global optimal particles can enhance the social learning ability of particles, as shown in Equation (19):

$$v_{i,t+1} = \omega \cdot v_{i,t} + r_1 \cdot \text{rand}() \cdot (LB_{i,t} - x_{i,t}) + r_2 \cdot \text{rand}() \cdot (GB_{local,i,t} - x_{i,t}) \quad (19)$$

where $GB_{local,i,t}$ refers to the best position of all particles after using LSS at iteration t . It is not hard to see that Equation (19) is the modification of Equation (15). According to the characteristics of OWFD and APSO, a new LSS is proposed in this paper. As far as we know, previous scholars mainly applied LSS for OWF micro-siting [35–37], then our work is the first to present a LSS to solve the CCLOP.

The mechanism of the proposed LSS can be explained as: randomly change the value of one dimension of the global optimal particle position. If the cable connection layout corresponding to the new particle benefits the objective function, it will replace the original global optimal particle, otherwise, it will be re-executed until the number of local search iteration reaches the predefined limit. Since the particle position includes the connection indexes and the CTIN indexes, the proposed LSS can help optimize the cable connection and cable selection at the same time. Continue with the same example as shown in Figure 6, two cases of particle updating using LSS are shown in Figure 7.

As can be seen in Figure 7, there are in total two cases. In the first case, it is assumed that the LSS randomly selects the 5th connection index and changes its value to 1, and then the particle 2 positon [2,4,1,1,1,0,1,2,1,0] is obtained. Further, decoding the particle 2 positon, the cable connection layout of particle 2 is shown in the bottom left of Figure 7. It can be seen from the figure that the cable connection layouts of particle 1 and particle 2, after triggering the LSS, the branch (4,5) becomes branch (1,5). In the second case, supposing that the LSS randomly selects the 1st CTIN index, and changes the value on this position to 1 to get the new particle 3 position [2,4,1,1,2,1,1,2,1,0]. Similarly, decoding the particle 3 positon, the cable connection layout of particle 3 is shown in the bottom right of Figure 7. It can be seen from the cable connection layout after two particle codec that after LLS, the cable type of branch (1,2) changes from type 1 to type 2.

It is worth noting that the above two cases only generate candidate particles. The information of the global optimal particles will never update except that the LSS helps generate a better solution. Therefore, this strategy can not only retain the original global search ability of APSO, but also improve the local searching ability of the algorithm. The performance of LSS in finding a better solution will be further demonstrated in the simulation.

3.3. Optimization Framework

In this paper, we use the V-APSO-LS algorithm to solve the CCLOP for an OWFD. The optimization framework is shown in Figure 8. As can be seen in Figure 8, the algorithm starts with initializing Voronoi distance matrix which is generated as described in Section 3.2.1. According to the locations of the WTs and OS, the particle population and its

related parameters are initialized in the next step. After importing such information into fitness function, the fitness value of each particle is obtained followed by the procedure in Section 3.2.2, which is the basis of the later fitness comparison. Further, the position and velocity of particles and their corresponding fitness values are updated, and the current global optimal solution will be updated via the LSS in Section 3.2.3. The above steps will not be terminated until the stop criteria are met. Finally, the optimal cable layout and the corresponding costs will be obtained.

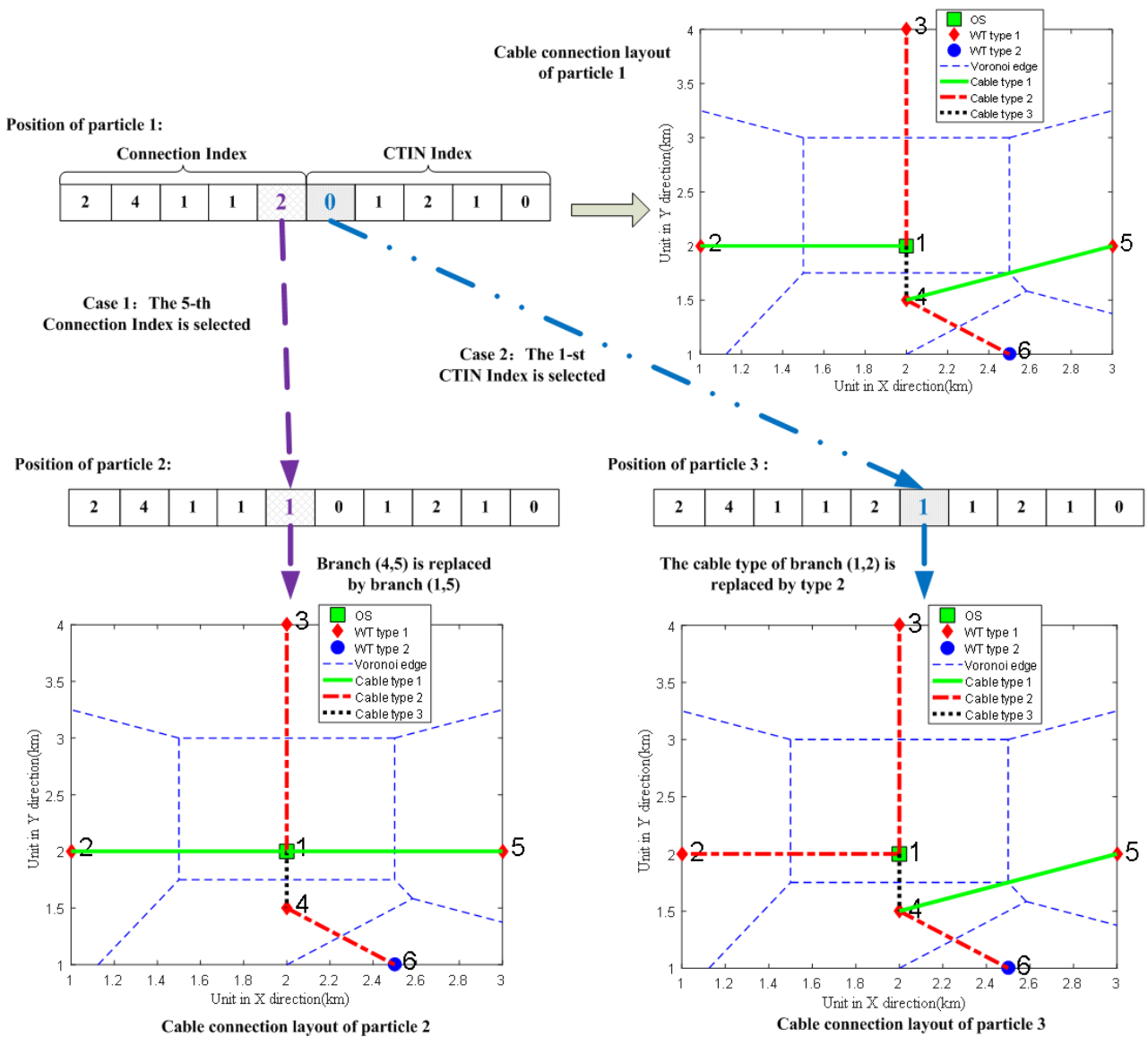


Figure 7. LSS for OWFD.

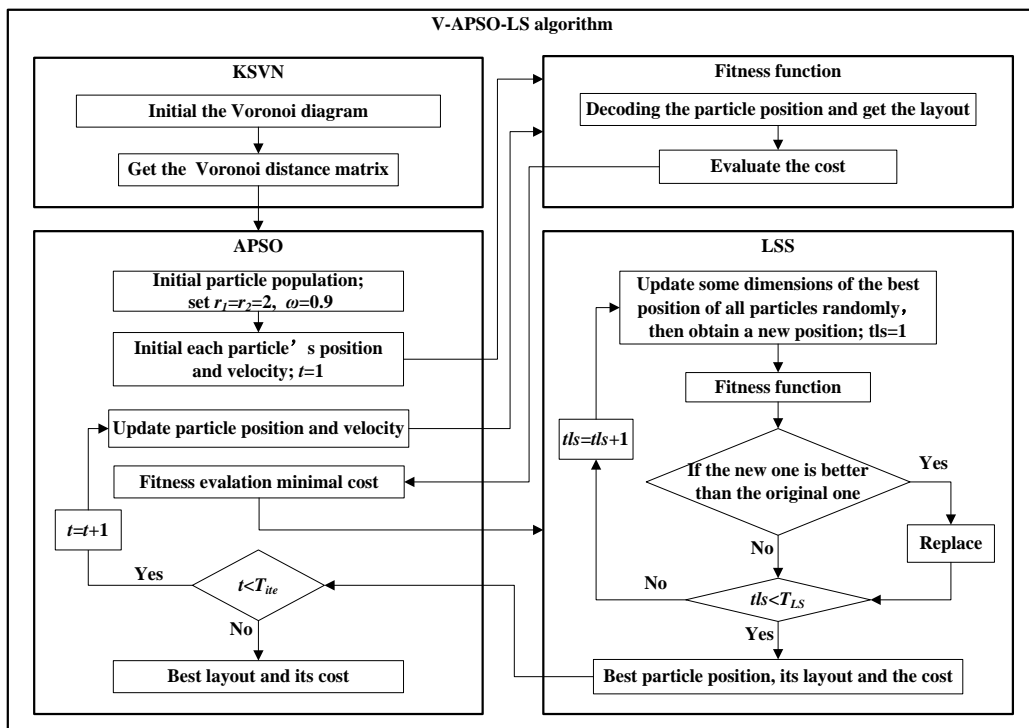


Figure 8. Optimization framework of V-APSO-LS.

4. Case Study

In this section, a reference OWFD is introduced at first. Then, two scenarios are presented with detailed results comparison and discussion at the end. In addition, the simulation software is MatLab, and the experimental simulation environment is Windows 10 OS, Intel Corei7-6800K CPU@3.40 GHz, 16 GB RAM.

4.1. Reference Wind Farm

In this work, an offshore wind farm with one OS and 72 WTs was selected. There are three types of WTs in this wind farm, with the rated power of 3 MW, 3.3 MW and 6.4 MW respectively. The positions of the OS and WTs are already known. The technical and economic information related to the wind farm is shown in Table A1 while the cable specifications are shown in Table A2. In addition, all cables are 3-core cross-linked polyethylene AC cables.

4.2. Simulation Results and Discussion

In this section, two scenarios are presented to validate the proposed method. According to our many trials, when the number of iterations is set to 150 and the population size is set to 500, the algorithm can solve CCLOP of OWFD better. Then, to ensure the comparison fairness, the number of iterations of each algorithm is set to 150 and the population size of each algorithm is set to 500, while each algorithm is run 10 times independently. The best solution among the 10 trials is selected as the optimal cable connection scheme, the result of which will be discussed and analyzed at last.

4.2.1. Scenario I

In this scenario, two optimization models for solving CCLOP are adopted and solved by the proposed V-APSO-LS. The first model (Model 1) is a cable connection layout scheme constructed on the minimum cross-sectional area cable selection rule, that is, cables with the small cross-sectional areas but satisfying Equation (11) are selected as far as possible for layout which is the model proposed in [7]. The second model (Model 2) further considers

the impact of the CELC on the cable type selection, which is the model proposed in Section 2. The simulation results are shown in Figure 9.

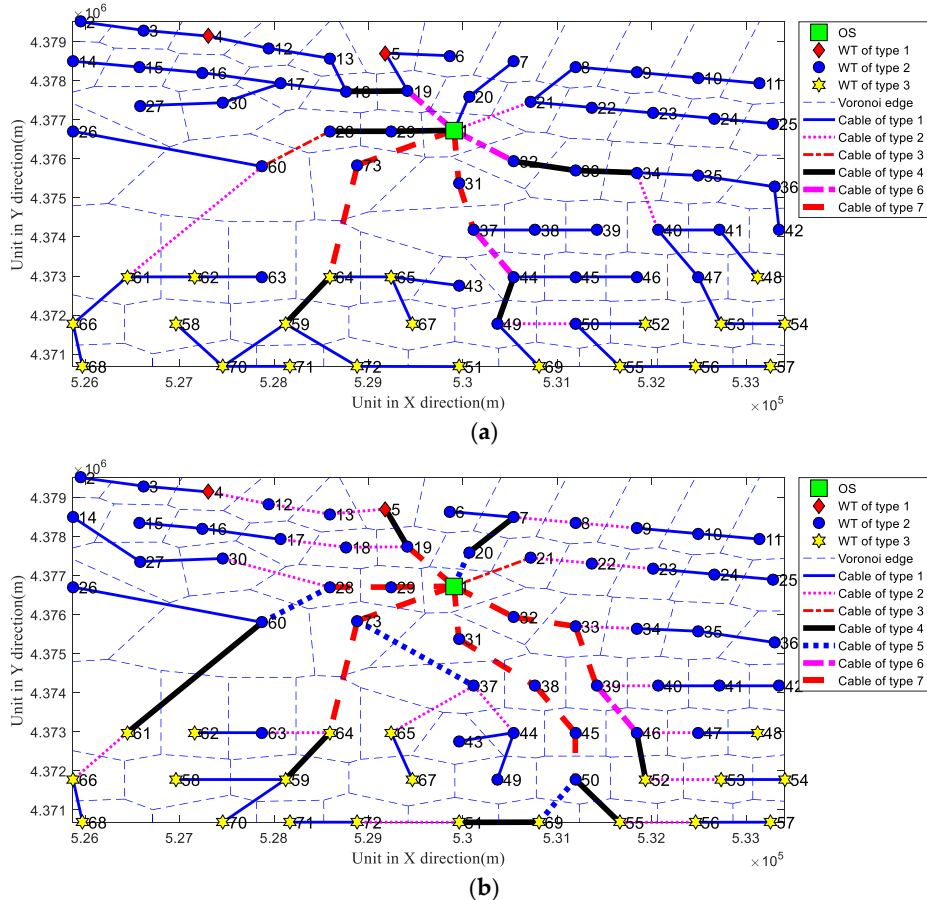


Figure 9. Optimized cable connection scheme. (a) Optimized layout of Model 1 obtained by V-APSO-LS; (b) Optimized layout of Model 2 obtained by V-APSO-LS.

It can be seen in Figure 9, no crossed cables appear in either the layout obtained by Model 1 or Model 2. Six kinds of cables are used for Model 1 case while in Model 2 seven kinds of cables are used. Compared with Figure 9a, there are fewer blue cables in Figure 9b which shows that Model 2 chooses more cables with the larger cross-sectional area. The reason is that Model 2 considering the influence of CELC. To highlight the difference, the branches with the larger cross-sectional area are shown in Figure 10.

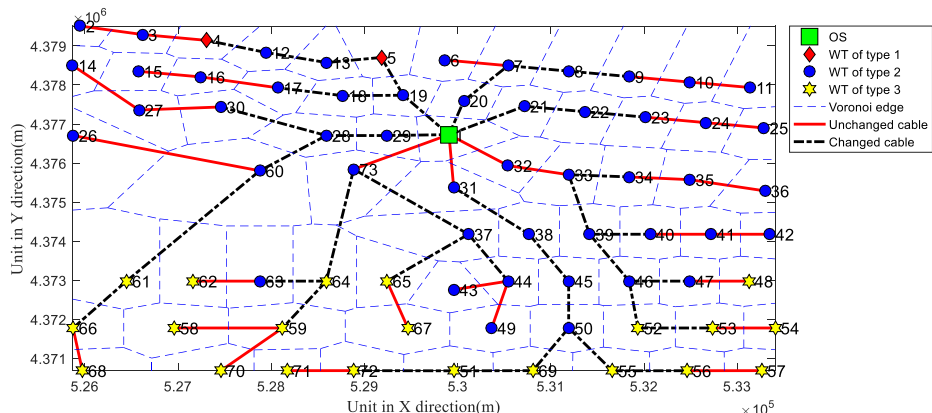


Figure 10. Optimized layout of Model 2 and highlighted the cables which changed the cross-section.

The statistic results for running each model using V-APSO-LS are shown in Figure 11. As can be seen from Figure 11, the optimal solutions of Model 1 and Model 2 appear in the 8th and 2nd experiments respectively. Compared to Model 1, Model 2 gives a better cable connection layout. In order to better understand the advantages and disadvantages of the two models, the detailed cost information of the optimal cable connection layout obtained by each model is shown in Table 1.

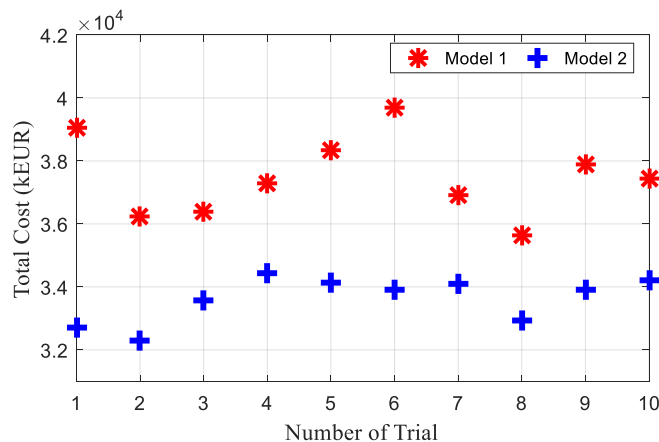


Figure 11. Ten trails for layout optimization of Model 1 and Model 2 obtained by V-APSO-LS.

Table 1. Simulation results of Model 1 and Model 2.

Item	Model 1	Model 2
CAPEX (kEUR)	18,983.49	22,014.29
CELC (kEUR)	16,666.47	10,272.63
Total cost (kEUR)	35,649.96	32,286.92

It can be seen from Table 1 that the cable procurement cost of Model 2 is 3030.80 kEUR more expensive than that of Model 1. However, the energy consumption cost of Model 2 is only 10,272.63 kEUR, which is 38.36% less than that of Model 1. As a result, the total cost of Model 2 is 9.43% lower than that of Model 1. Although more expensive cables are purchased in Model 2, the savings in CELC lead to a lower overall cost compared with the situation of using Model 1.

4.2.2. Scenario II

In order to verify the proposed V-APSO-LS, and the effect of using KSVN and LSS, the other three algorithms are used to solve Model 2 and compared with V-APSO-LS. The first algorithm, Voronoi diagram-based adaptive particle swarm optimization (V-APSO) is constructed by V-APSO-LS without using LSS. The second adaptive particle swarm optimization minimum spanning tree (APSO-MST) algorithm is from [7]. The third algorithm, Voronoi diagram-based wild goats algorithm with local search (V-WGA-LS), is to replace the APSO in V-APSO-LS with wild goats algorithm proposed in [38], but still, retain KSVN and LSS. The 10 trials results of the four algorithms are shown in Figure 12, and the average computational times of V-APSO-LS, V-APSO, APSO-MST and V-WGA-LS are 1284 s, 1176 s, 1522 s, 2452 s, respectively.

As can be seen from Figure 12, the optimal solutions of V-APSO-LS, V-APSO, APSO-MST and V-WGA-LS appeared at the 2nd, 3rd, 6th and 5th times respectively. The results obtained by the APSO-MST are the worst. In contrast, the V-APSO finds the best solution. The optimized layout obtained by V-APSO, APSO-MST and V-WGA-LS are shown in Figure 13. Then, the fitness value corresponding to each iteration is shown in Figure 14.

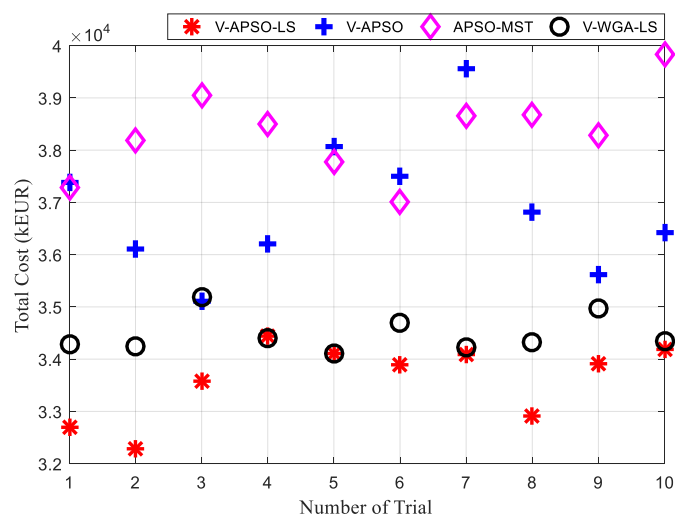


Figure 12. Ten trails for layout optimization of Model 2 obtained by V-APSO-LS, V-APSO, APSO-MST and V-WGA-LS.

As can be seen from Figure 14, the result obtained by the V-APSO with KSVN is better than the result obtained by the APSO-MST which shows the rationality of using the Voronoi distance to judge the proximity relations between points in the layout. It is worthy of note that after the 10th iteration, the convergence rate of V-APSO becomes slower. Furthermore, V-APSO-LS with LSS is much better than V-APSO after 10 iterations. It is verified that the LSS proposed in this paper can greatly enhance the searching ability of the APSO.

In addition, after the 10th iteration, the trace of the convergence of V-WGA-LS is similar to that of V-APSO-LS. However, the convergence speed of V-APSO-LS is faster while retaining a better solution which shows the superiority of the APSO than the wild goats algorithm. The detailed cost comparison of the optimal cable connection layout obtained by each algorithm is shown in Table 2.

Table 2. The best, mean and worst solutions obtained by different algorithms in 10 trials.

	Item	CAPEX (kEUR)	CELC (kEUR)	Total Cost (kEUR)
Best Solution	V-APSO-LS	22,014.29	10,272.63	32,286.92
	V-APSO	21,081.63	14,026.23	35,107.86
	APSO-MST	19,791.80	17,208.97	37,000.77
	V-WGA-LS	21,869.70	12,241.77	34,111.47
Mean Solution	V-APSO-LS	22,970.34	10,643.30	33,613.64
	V-APSO	21,015.19	15,862.99	36,878.18
	APSO-MST	19,622.79	18,700.80	38,323.59
	V-WGA-LS	22,065.20	12,412.29	34,477.49
Worst Solution	V-APSO-LS	23,923.75	10,514.20	34,437.95
	V-APSO	22,823.75	16,742.74	39,566.49
	APSO-MST	19,360.48	20,470.10	39,830.58
	V-WGA-LS	22,324.53	12,855.72	35,180.25

As can be seen in Table 2, compared with the best, mean and worst solutions of the algorithms respectively, the CAPEXes obtained by the APSO-MST are always the lowest, whereas due to the higher CELCs, the total costs are the largest. Therefore, the accuracy and stability of the V-APSO-LS are better than the other three algorithms. Furthermore, the V-APSO-LS achieves the best solution which is 8.04%, 12.74% and 5.35% lower than the solutions found by the V-APSO, APSO-MST, and V-WGA-LS respectively.

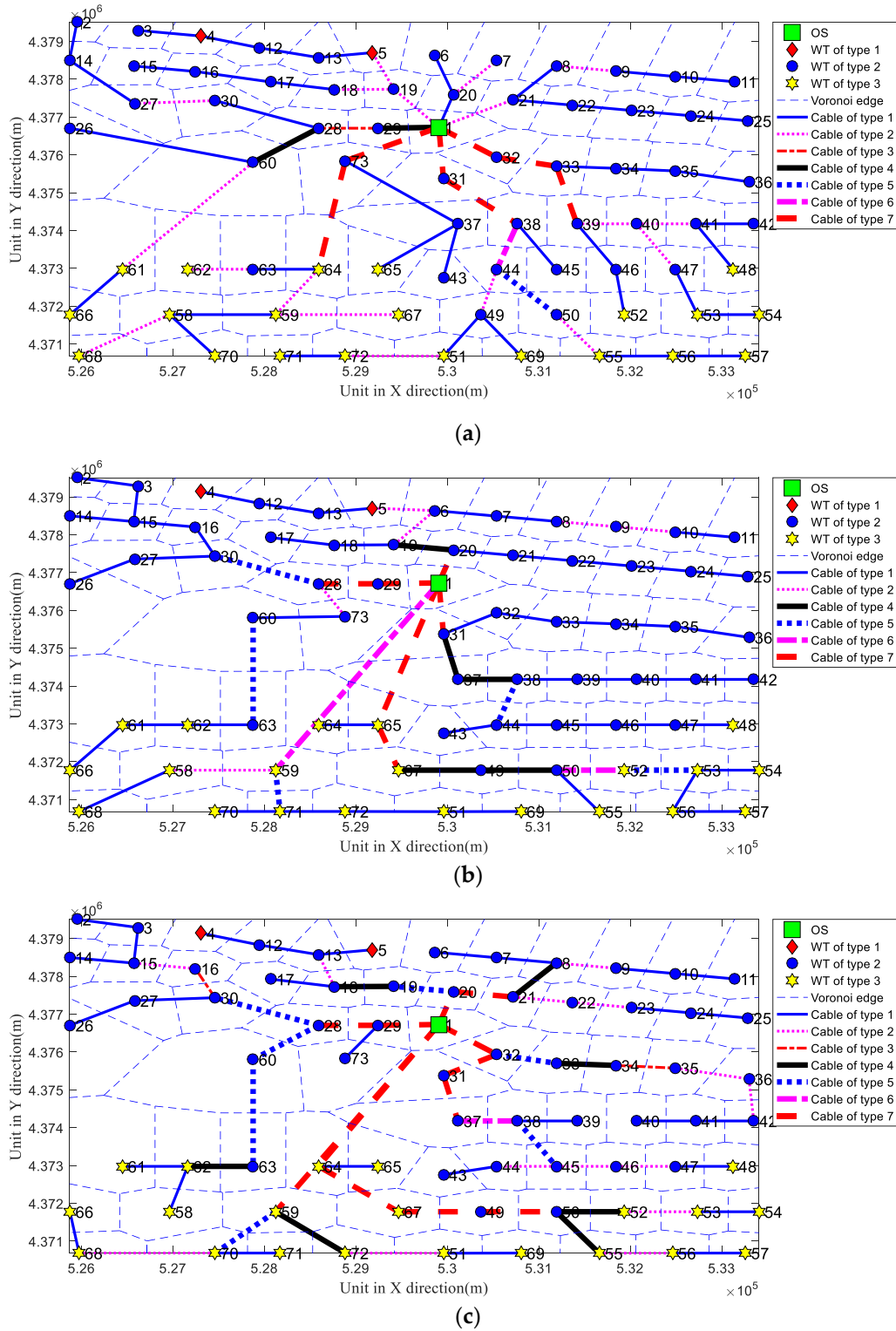


Figure 13. Optimized cable connection scheme. (a) Optimized layout obtained by V-APSO; (b) Optimized layout obtained by APSO-MST; (c) Optimized layout obtained by V-WGA-LS.

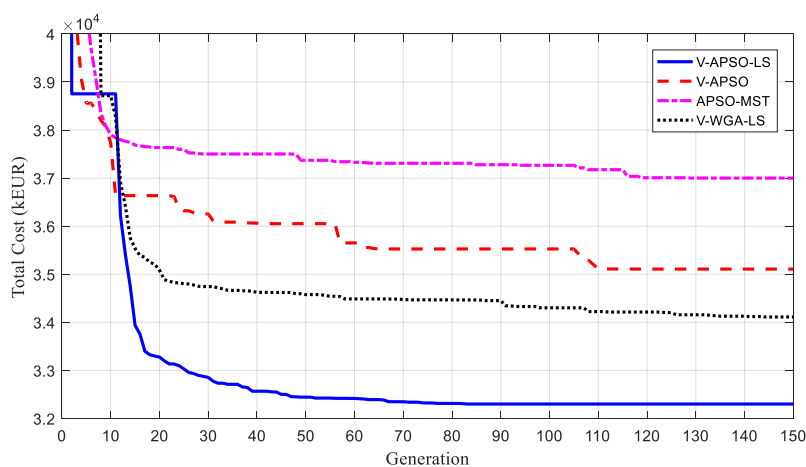


Figure 14. Total cost corresponding to each generation.

5. Conclusions

In this paper, the influence of energy loss on the overall cable connection structure economy is fully considered. Aiming at minimizing the total cost of OWFD, a CCLOP model based on OWFD is established. In order to get an optimized result, this paper proposes a V-APSO-LS which takes APSO as the core and adopts the KSVN and LLS to enhance the optimized performance. In the simulation experiment of Scenario I, this paper proves that fully considering the impact of CELC on the overall cable connection layout is conducive to reducing the total cost of OWFD during the operation period. Furthermore, in scenario II, the layout scheme of V-APSO-LS is superior to V-APSO, APSO-MST and V-WGA-LS, which proves the effectiveness of the algorithm and the optimization strategy proposed in this paper. Therefore, this paper provides effective theoretical guidance and technical support for the cable connection layout optimization of OWFD.

In the future, CCLOP of large-scale OWFD can be established and optimized considering the number and location of offshore substations, and then compared with the used industrial layout. At the same time, more optimization strategies is promising to be adopted for improve the ability of the intelligent algorithm in solving the complex combinational optimization tasks in terms of offshore wind energy.

Author Contributions: Writing—original draft preparation, Y.Q.; writing—review and editing, P.H.; review and editing, G.L., Z.Y., G.Y. and Z.D.; writing—original draft preparation, R.J. All authors have read and agreed to the published version of the manuscript.

Funding: This research was funded by Key Project in Higher Education of Guangdong Province, China under grant No. 2020ZDZX3030, Young Innovation Talents Project in Higher Education of Guangdong Province, China under under No. 2018KQNCX333, National Science Foundation of China under grants 52077213 and 62003332, Natural Science Foundation of Guangdong (No. 2018A030313755).

Institutional Review Board Statement: Not applicable.

Informed Consent Statement: Not applicable.

Data Availability Statement: The data presented in this study are available on request from the corresponding author.

Acknowledgments: This research was funded by Key Project in Higher Education of Guangdong Province, China under grant No. 2020ZDZX3030, Young Innovation Talents Project in Higher Education of Guangdong Province, China under under No. 2018KQNCX333, National Science Foundation of China under grants 52077213 and 62003332, Natural Science Foundation of Guangdong (No. 2018A030313755).

Conflicts of Interest: The authors declare no conflict of interest.

Abbreviations

OWF	Offshore Wind Farm	$H_{G_T,m}$	Number of the WTs that transmit their power through the branch m of G_T
OWFD	Offshore Wind Farm with Diverse Wind Turbine Types	h	Index of the WTs that transmit their power through one branch
OS	Offshore Substation	$\varphi_{G_T,m,p}$	If branch m of G_T uses type p cable, $\varphi_{G_T,m,p} = 1$, otherwise $\varphi_{G_T,m,p} = 0$.
WT	Wind Turbine	$\delta_{G_T,q,h}$	If the h th WT transmits its power through the branch m of G_T is WT type q , $\delta_{G_T,q,h} = 1$, otherwise $\delta_{G_T,q,h} = 0$.
CAPEX	Capital Expenditure	T	Lifetime of the wind farm [Year]
CELC	Cable Energy Losses Cost	C_{loss}	Unit cost of energy loss of cable [EUR/MWh]
CCLOP	Cable Connection Layout Optimization Problem	ψ_Δ	Duration time of peak energy loss [h]
MST	Minimum Spanning Tree	ψ	Power factor
APSO	Adaptive Particle Swarm Optimization	η	Interest rate
APSO-MST	Adaptive Particle Swarm Optimization Minimum Spanning Tree	$Z_{CAPEX,G_T,m,p}$	Cost of CAPEX of branch m with cable type p in G_T [EUR]
KSVN	K-ring Shaped Voronoi Neighbor	Z_{CAPEX,G_T}	Total cost of CAPEX in G_T [EUR]
LSS	Local Search Strategy	$Z_{CELC,G_T,m,p}$	Cable energy losses of branch m with cable type p in G_T [MWh]
CTIN	Cable Type Incremental Number	Z_{CELC,G_T}	Cost of CELC in G_T [EUR]
V-APSO-LS	Voronoi Diagram based Adaptive Particle Swarm Optimization with Local Search	$Z_{min,total}$	Total cost for the multiple wind turbine types offshore wind farm [EUR]
V-APSO	Voronoi Diagram based Adaptive Particle Swarm Optimization	$V_{WT,m}$	The vertex m which notes WT m in V_{WT}
V-WGA-LS	Voronoi Diagram based Wild Goats Algorithm with Local Search	$F_{G_T,V_{OS,in}}$	Number of Feeders in G_T
G	an undirected graph	$F_{G_T,V_{WT,m,in}}$	Number of input cables of WT m in G_T
G_T	Sub-graph belongs to G	$F_{G_T,V_{WT,m,out}}$	Number of output cables of WT m in G_T
V	Vertex set in G	B_{m1}, B_{m2}	Branch $m1$ and branch $m2$ in B_T
B	All branches that connect V in G	i	Index of particles
B_T	All branches that connect V in G_T	T_{ite}	Number of iterations
W	Weight of each branch in G	t	Index of iterations
W_T	Weight of each branch in G_T	$x_{i,t}, x_{i,t+1}$	Position of particle i at iteration t and $t + 1$
V_{OS}	The vertex which notes the OS in V	$v_{i,t}, v_{i,t+1}$	Velocity of particle i at iteration t and $t + 1$,
V_{WT}	The vertex set which notes WTs in V	$LB_{i,t}$	Best position of particle i at iteration t
M	Number of wind turbines	$GB_{i,t}$	Best position of all particles at iteration t
P	Number of cable types	ω	Inertia weight
Q	Number of WT types	r_1, r_2	Learning factors
M	Index of a branch in G_T ; Index of WT in V_{WT} ; Index of the dimension of the particle position	μ	Evolutionary factor
R	Index of wind farm operation period	d_{avg}	Mean distance from the global best particle to the others
P	Index of cable type	d_{min}, d_{max}	Minimal and maximum mean distances from one particle to the others
Q	Index of WT type	E_1, E_2	Site E_1 and site E_2 in the Voronoi diagram
C_p	Unit cost of cable type p (EUR/m)	$VR(E_1), VR(E_2)$	Voronoi regions of site E_1 and site E_2
R_p	Unit resistance of cable type p (Ω/km)	$KN(E_1, k)$	The k -ring shaped Voronoi neighbors set of site E_1
$I_{max,p}$	Current-carrying capacity of cable type p (A)	$GB_{local,i,t}$	Best position of all particles after using LSS at iteration t
$P_{rate,q}$	Rated active power of WT type q (MW)	T_{LS}	Maximum attempts of local search
$U_{rate,q}$	Rated voltage of WT type q (kV)	t_{ls}	The t_{ls} th attempt of T_{LS}
$I_{rate,q}$	Rated current of WT type q (A)	AM	Adjacency matrix
$L_{G_T,m}$	Length of the branch m in G_T (m)	SAM	Sorted-adjacency matrix
$I_{G_T,m,p}$	Actual current in branch m with cable type p in G_T (A)		

Appendix A

Table A1. Other basic technical and economic data of the wind farm.

Item	Value	Item	Value
$U_{rate,q}$	66.0 kV	η	0.049
T	25 Year	ψ_Δ	2608 h
$\cos \psi$	0.95	C_{loss}	109.055 EUR/MWh

Table A2. Basic technical and economic data for 66 KV, XRUHAKXS cable.

Type No.	Sectional Area	Price (EUR/m)	Resistance (Ω/km)	Ampacity (A)
T1	95	233.634	0.2500	260
T2	120	251.340	0.1458	315
T3	150	271.355	0.1250	350
T4	185	301.633	0.0970	428
T5	240	343.844	0.0729	440
T6	300	382.462	0.0600	520
T7	400	443.918	0.0437	600

References

- Chen, Y.; Dong, Z.; Meng, K.; Luo, F.; Yao, W.; Qiu, J. A novel technique for the optimal design of offshore wind farm electrical layout. *J. Mod. Power Syst. Clean Energy* **2013**, *1*, 258–263. [[CrossRef](#)]
- Qi, Y.; Hou, P.; Yang, L.; Yang, G. Simultaneous optimisation of cable connection schemes and capacity for offshore wind farms via a modified bat algorithm. *Appl. Sci.* **2019**, *9*, 265. [[CrossRef](#)]
- Hou, P.; Hu, W.; Soltani, M.; Chen, C.; Chen, Z. Combined optimization for offshore wind turbine micro siting. *Appl. Energy* **2017**, *189*, 271–282. [[CrossRef](#)]
- Hou, P.; Hu, W.; Soltani, M.; Chen, Z. Optimized placement of wind turbines in large-scale offshore wind farm using particle swarm optimization algorithm. *IEEE Trans. Sustain. Energy* **2015**, *6*, 1272–1282. [[CrossRef](#)]
- Ling-ling, H.; Ning, C.; Hongyue, Z.; Yang, F. Optimization of large-scale offshore wind farm electrical collection systems based on improved FCM. In Proceedings of the International Conference on Sustainable Power Generation and Supply (SUPERGEN 2012), Hangzhou, China, 8–9 September 2012; pp. 1–6.
- Huang, L.; Yang, F.; Guo, X. Optimization of electrical connection scheme for large offshore wind farm with genetic algorithm. In Proceedings of the 2009 International Conference on Sustainable Power Generation and Supply, Supergen, Nanjing, China, 6–7 April 2009; pp. 1–4.
- Hu, W.; Chen, Z.; Hou, P. Optimisation for offshore wind farm cable connection layout using adaptive particle swarm optimisation minimum spanning tree method. *IET Renew. Power Gener.* **2016**, *10*, 694–702. [[CrossRef](#)]
- Chen, Y.; Dong, Z.Y.; Meng, K.; Luo, F.; Xu, Z.; Wong, K.P. Collector system layout optimization framework for large-scale offshore wind farms. *IEEE Trans. Sustain. Energy* **2016**, *7*, 1398–1407. [[CrossRef](#)]
- Li, D.D.; He, C.; Fu, Y. Optimization of internal electric connection system of large offshore wind farm with hybrid genetic and immune algorithm. In Proceedings of the International Conference on Electric Utility Deregulation and Restructuring and Power Technologies, Nanjing, China, 6–9 April 2008; pp. 2476–2481.
- Gonzalez-Longatt, F.M.; Wall, P.; Regulski, P.; Terzija, V. Optimal electric network design for a large offshore wind farm based on a modified genetic algorithm approach. *IEEE Syst. J.* **2012**, *6*, 164–172. [[CrossRef](#)]
- Lumbrieras, S.; Ramos, A.; Sanchez-Martin, P. Offshore wind farm electrical design using a hybrid of ordinal optimization and mixed-integer programming. *Wind Energy* **2015**, *18*, 2241–2258. [[CrossRef](#)]
- Wędzik, A.; Siewierski, T.; Szypowski, M. A new method for simultaneous optimizing of wind farm's network layout and cable cross-sections by MILP optimization. *Appl. Energy* **2016**, *182*, 525–538. [[CrossRef](#)]
- Chowdhury, S.; Zhang, J.; Messac, A.; Castillo, L. Optimizing the arrangement and the selection of turbines for wind farms subject to varying wind conditions. *Renew. Energy* **2013**, *52*, 273–282. [[CrossRef](#)]
- Abdulrahman, M.; Wood, D. Investigating the Power-COE trade-off for wind farm layout optimization considering commercial turbine selection and hub height variation. *Renew. Energy* **2017**, *102*, 267–278. [[CrossRef](#)]
- Chowdhury, S.; Zhang, J.; Messac, A.; Castillo, L. Unrestricted wind farm layout optimization (UWFLO): Investigating key factors influencing the maximum power generation. *Renew. Energy* **2012**, *38*, 16–30. [[CrossRef](#)]
- Feng, J.; Shen, W.Z. Design optimization of offshore wind farms with multiple types of wind turbines. *Appl. Energy* **2017**, *205*, 1283–1297. [[CrossRef](#)]
- Chen, K.; Song, M.X.; Zhang, X.; Wang, S.F. Wind turbine layout optimization with multiple hub height wind turbines using greedy algorithm. *Renew. Energy* **2016**, *96*, 676–686. [[CrossRef](#)]

18. Gong, X.; Kuenzel, S.; Pal, B.C. Optimal wind farm cabling. *IEEE Trans. Sustain. Energy* **2018**, *9*, 1126–1136. [[CrossRef](#)]
19. Dahmani, O.; Bourguet, S.; Machmoum, M.; Guerin, P.; Rhein, P.; Josse, L. Optimization of the connection topology of an offshore wind farm network. *IEEE Syst. J.* **2015**, *9*, 1519–1528. [[CrossRef](#)]
20. Jin, R.; Hou, P.; Yang, G.; Qi, Y.; Chen, C.; Chen, Z. Cable routing optimization for offshore wind power plants via wind scenarios considering power loss cost model. *Appl. Energy* **2019**, *254*, 113719. [[CrossRef](#)]
21. Duczmal, L.H.; Moreira, G.J.P.; Burgarelli, D.; Takahashi, R.H.C.; Magalhaes, F.C.O.; Bodevan, E.C. Voronoi distance based prospective space-time scans for point data sets: A dengue fever cluster analysis in a southeast Brazilian town. *Int. J. Health Geogr.* **2011**, *10*, 29. [[CrossRef](#)]
22. Fang, Z.; Tu, W.; Li, Q.; Shaw, S.-L.; Chen, S.; Chen, B.Y. A Voronoi neighborhood-based search heuristic for distance/capacity constrained very large vehicle routing problems. *Int. J. Geogr. Inf. Sci.* **2013**, *27*, 741–764. [[CrossRef](#)]
23. Fang, Z.; Li, Q.; Shaw, S.-L.; Chen, B.; Chen, B. A bi-level Voronoi diagram-based metaheuristic for a large-scale multi-depot vehicle routing problem. *Transp. Res. Part Logist. Transp. Res.* **2014**, *61*, 84–97. [[CrossRef](#)]
24. Fischetti, M.; Pisinger, D. Optimizing wind farm cable routing considering power losses. *Eur. J. Oper. Res.* **2018**, *270*, 917–930. [[CrossRef](#)]
25. Kennedy, J.; Eberhart, R. Particle swarm optimization. In Proceedings of the ICNN’95—International Conference on Neural Networks, Perth, WA, Australia, 27 November–1 December 1995; Volume 4, pp. 1942–1948.
26. Kennedy, J. The particle swarm: Social adaptation of knowledge. In Proceedings of the 1997 IEEE International Conference on Evolutionary Computation (ICEC ‘97), Indianapolis, IN, USA, 13–16 April 1997; pp. 303–308.
27. Zhan, Z.-H.; Zhang, J.; Li, Y.; Chung, H.S.-H. Adaptive particle swarm optimization. *IEEE Trans. Syst. Man Cybern. Part (Cybern.)* **2009**, *39*, 1362–1381. [[CrossRef](#)] [[PubMed](#)]
28. Hou, P.; Hu, W.; Zhang, B.; Soltani, M.; Chen, C.; Chen, Z. Optimised power dispatch strategy for offshore wind farms. *IET Renew. Power Gener.* **2016**, *10*, 399–409. [[CrossRef](#)]
29. Rania, H.; Babak, C.; Olivier, W. A comparison of particle swarm optimization and the genetic algorithm. In Proceedings of the 46th AIAA/ASME/ASCE/AHS/ASC Structures, Structural Dynamics and Materials Conference, Austin, TX, USA, 18–21 April 2005; pp. 1–13.
30. Aurenhammer, F. Voronoi diagrams—A survey of a fundamental geometric data structure. *ACM Comput. Surv.* **1991**, *23*, 345–405. [[CrossRef](#)]
31. Stoyan, D. Spatial tessellations: Concepts and applications of voronoi diagrams. *Biom. J.* **2010**, *36*, 146. [[CrossRef](#)]
32. Chen, J.; Li, C.; Li, Z.; Gold, C. A Voronoi-based 9-intersection model for spatial relations. *Int. J. Geogr. Inf. Sci.* **2001**, *15*, 201–220. [[CrossRef](#)]
33. Fischetti, M.; Monaci, M. Proximity search heuristics for wind farm optimal layout. *J. Heuristics* **2016**, *22*, 459–474. [[CrossRef](#)]
34. Wagner, M.; Day, J.; Neumann, F. A fast and effective local search algorithm for optimizing the placement of wind turbines. *Renew. Energy* **2013**, *51*, 64–70. [[CrossRef](#)]
35. Wan, C.; Wang, J.; Yang, G.; Gu, H.; Zhang, X. Wind farm micro-siting by Gaussian particle swarm optimization with local search strategy. *Renew. Energy* **2012**, *48*, 276–286. [[CrossRef](#)]
36. Abdelsalam, A.M.; El-Shorbagy, M.A. Optimization of wind turbines siting in a wind farm using genetic algorithm based local search. *Renew. Energy* **2018**, *123*, 748–755. [[CrossRef](#)]
37. Carrabs, F.; Cerrone, C.; Pentangelo, R. A multiethnic genetic approach for the minimum conflict weighted spanning tree problem. *Networks* **2019**, *74*, 134–147. [[CrossRef](#)]
38. Shefaei, A.; Mohammadi-Ivatloo, B. Wild goats algorithm: An evolutionary algorithm to solve the real-world optimization problems. *IEEE Trans. Ind. Inform.* **2018**, *14*, 2951–2961. [[CrossRef](#)]